IEEE Access
Multidisciplinary ⋮ Rapid Review ⋮ Open Access Journal

Received 11 May 2023, accepted 27 May 2023, date of publication 9 June 2023, date of current version 19 June 2023.

Digital Object Identifier 10.1109/ACCESS.2023.3284466

RESEARCH ARTICLE

Sensorless Control of a Single-Phase AC–DC Boost Converter Without Measuring Input Voltage and Current

MEHDI TAVAN[1], KAMRAN SABAHI[2], MAHDI SHAHPARASTI[3], (Senior Member, IEEE), AMIN HAJIZADEH[4], (Senior Member, IEEE), MOHSEN SOLTANI[4], (Senior Member, IEEE), AND MEHDI SAVAGHEBI[5,6], (Senior Member, IEEE)

[1]Department of Electrical Engineering, Nour Branch, Islamic Azad University, Nour 4641859557, Iran
[2]Department of Engineering Sciences, University of Mohaghegh Ardabili, Namin 5619911367, Iran
[3]School of Technology and Innovations, University of Vaasa, 65200 Vaasa, Finland
[4]AAU Energy, Aalborg University, 6700 Esbjerg, Denmark
[5]Department of Mechanical and Electrical Engineering, University of Southern Denmark, 5230 Odense, Denmark
[6]Department of Engineering Technology, Technical University of Denmark (DTU), 2750 Ballerup, Denmark

Corresponding author: Mehdi Tavan (m.tavan@srbiau.ac.ir)

ABSTRACT It is well-known that the accurate measurement of input voltage and current, as the feedforward and feedback terms, plays a crucial role in the nonlinear controller design for power factor compensation of an AC-DC boost converter. This paper addresses the problem of the simultaneous estimation of the input voltage and current from the output voltage in a *full-bridge* AC-DC boost converter. In the lossless model of the system, those variables are unobservable from the output voltage when the control input is zero. To overcome this, the system dynamics are *immersed* in a proper form by a new filtered transformation. The phase and amplitude of the input voltage, along with the input current, are globally estimated from the output voltage by a fifth-dimensional estimator. Unlike some existing results, the stability of the proposed estimator does not rely on *a priori* knowledge about the parasitic resistances and is guaranteed exponentially under the persistence of excitation conditions on the control signal. An application of the proposed estimator is presented in conjunction with a dynamic controller to form a sensorless control algorithm that does not require any sensor on the input side and controls the system only by the feedback from the output voltage. Processor-in-the-loop (PIL) studies conducted by OPAL-RT OP 5700 are used to assess the performances of the proposed estimator and controller.

INDEX TERMS AC–DC power converters, adaptive estimator, immersion and invariance technique, Lyapunov stability.

NOMENCLATURE

i	Input current
v_i	Input voltage
v	Output voltage
u	Control input
L	Inductance
C	Capacitance
G	Load conductance
E	v_i- amplitude
ω	v_i-angular frequency
ρ	v_i-phase
$\Delta\rho$	Phase difference between v_i and i
θ	Unknown vector
φ	Regressor vector
ι	Filtered transformation state
μ	Filtered regressor
ζ_1, ζ_2	Estimator states
κ, λ, Λ	Estimator gains
a, b, d, K	Controller gains
s	Steady state subscript
$\wedge$	Estimation superscript
$-$	Estimation error superscript

The associate editor coordinating the review of this manuscript and approving it for publication was Zheng Chen.

I. INTRODUCTION

AC-DC boost converters have widely been used for interfacing renewable energy sources to hybrid microgrids [1], [2], [3], flexible AC transmission systems [4], motor drive systems [5], LED drive systems [6], [7], etc. The average model of the converter in both *full-bridge* and *half-bridge* (interleaved) topologies has bilinear nature and is inherently nonlinear [8]. Also, the system is *nonminimum-phase* with respect to the output to be regulated, and since the states must be controlled only by one signal, the system is *underactuated,* too [9]. These features, besides the system applications, have made an attractive control problem from both theoretical and practical viewpoints. The control objective is to regulate, on average, the output voltage in some constant desired value with a near unity power factor on the input side [9].

For power factor compensation (PFC) purposes, the AC-DC boost converters are usually controlled by the current mode control (CMC) strategies [8], [9], [10], [11]. With respect to the *underactuation* property, the bidirectional control objectives are achieved in the CMC methodologies by phase and amplitude control of the input current. For a specified load and an arbitrary desired output voltage, the phase and amplitude of the desired input current are specified by their values in the input side voltage source [12]. With respect to the nonlinear nature of the system, achieving the desired values provides a nonlinear tracking control problem which requires the input voltage to provide the *feedforward* control signal [8], [9], [10], [11]. To stabilize the tracking error dynamics, *feedback* from the input current is essential, which improves the total harmonic distortion (THD) and power factor quality and indirectly improves output voltage regulation [13]. Hence, accurate measurement of the input voltage and current are vital for the nonlinear control design in boost converters such as [14], [15], [16], [17], [18].

The feedback control function depends on the input current sensor performance, which can be stymied by high temperature and measurement noise. Hence, the sensorless control of power converters has attracted a lot of attention in both industrial and academic applications. It is known that the use of these methods is cost-effective, reliable, and reduces performance sensitivity to measurement noise [19]. However, the bilinear nature of the commonly used power converter topologies makes the design process challenging, especially in the observer-based methodology. It is worth noting that the *lossless* model of the AC-DC boost converter belongs to the second-order bilinear systems group both of its states are not observable when the control signal is zero. It is worth pointing out that the *full-bridge* topology, which presents lower pollution in the line source than other topologies of the AC-DC boost converter [8], confronts the observability obstacle definitely due to its control input sign changes continuously. This poses a challenging problem for the state and parameter estimation. A few works have been reported to address this issue by the observer-based methodologies that are discussed in the following.

In [5], [6], and [20], *Luenberger-type* observers are employed to estimate the input current of an interleaved AC-DC boost converter. The observers construct an estimation error dynamics with asymptotic stability. The drawback is that the convergence rate of the estimation cannot improve arbitrarily and is limited to some bounds which depend on the system parameters. Also, *a priori* knowledge of the parasitic resistance of the system is required for such observers. An adaptive version of the Luenberger observer is proposed in [21] for estimating the input current and two parasitic parameters. However, the design procedure is stymied by the definition of an inappropriate Lyapunov function in which estimation convergence cannot be concluded from its time derivative (see Eq. (26) and (30) in [21]). Also, it is well known that the parametric convergence in the classical adaptive observer, such as the one proposed in [21], requires fulfilling an assumption known as *persistent excitation* (PE) condition (see Lemma B.2.3 of [22]). Another Luenberger-type adaptive observer is proposed in [23] to estimate the input current and the output load conductance. The adaptation law is derived based on *direct cancellation with matching* in a Lyapunov function candidate. The observer design procedure is hampered by the so-called *detectability obstacle* due to the existence of uncertainty in output dynamics (see [24] and Section 3.3 of [9]). A PE-like assumption on the states and control input is needed to guarantee the state and the parameter estimation in [23]. The detectability obstacle is tackled by an *immersion and invariance* (I&I) based observer design for a DC-DC boost converter with unknown load conductance in [25] which is extended to a class of DC-DC converters in [26]. Both of these works need to sense the input and output voltage. In [27], an output feedback controller is proposed for the DC-DC boost converter, which requires knowledge about output load conductance. The proposed algorithms in [25], [26], and [27] are based on a lossless model of the converter with considering the saturation of the control input. A generalized parameter estimation-based observer (GPEO) is designed for a class of converters, including boost converters, under a weaker convergence condition than PE in [28]. The design procedure imposes many degrees of freedom to provide the condition. Although there is no need for the value of the output load, *a priori* knowledge about the parasitic resistances and a measure of the input voltage is required for the foregoing method. The GPEO method is employed in [29] to form a sensorless control algorithm for a DC-DC boost converter. The proposed controller needs knowledge of the output load value and two sensors to measure the input and output voltages. A sliding mode observer is proposed in [30] with exponential current estimation for the three-phase AC-DC boost converter. A phase parasitic resistance, including the internal resistance of the voltage sources and the impedance of the switching elements, is considered in the model equations to facilitate the observer design procedure like to [5], [6], [20], [28], and [30]. Also, the current observers proposed in the foregoing

researches require a voltage sensor on the input side to extract the amplitude and phase of the AC source, in addition to the knowledge about the parasitic and load resistances. A nonlinear estimator based on filter transformation via dynamic matrix is presented for AC-DC boost converter in [31]. In this approach, an asymptotic estimation of the input current and voltage can be extracted from a ninth-dimensional observer under a non-square-integrability condition. Regardless of the observer order which is high and hard to implement, the convergence condition is hard to be verified for the dynamic matrix.

The problem of sensorless control, *i.e.*, voltage output feedback control, of the AC-DC boost converter, using a single output voltage sensor has been addressed in [19]. A manifold is extracted from the instantaneous power balancing equality for the unity power factor in the lossless model of the system. Along the trajectories of the system on the manifold, changes of the unavailable states are locally computed in terms of changes in the DC link voltage. Although using the lossless model relaxes the need for *a priori* knowledge about parasitic resistance, the input current and voltage estimation are hampered by the observability obstacle when the control signal is zero. Also, a dynamic transformation is required to transform the system model to a proper adaptive observer form. Unlike [19], in this paper, a nonlinear, globally convergent, and robust estimator is designed for an AC-DC full-bridge boost converter to estimate the input current and the input voltage from the output voltage. Instrumental for the construction of the estimator is the use of I&I-based filtered transformation that poses a lower degree of freedom in comparison to the one presented in [31] and the GPEO design in [28]. Besides reducing the number of sensors, the proposed estimator relaxes the knowledge about the parasitic resistance value that is instrumental in the creation of a globally convergent observer in [5], [6], [20], [28], and [30]. An application of the estimator is presented in conjunction with a dynamic controller reported in [9]. The controller is reinforced to circumvent the singularity problem, which can occur when the estimated parameters are replaced instead of the real ones. As a result, a sensorless control algorithm is proposed which does not require any sensor on the input side and controls the system only by the feedback from the output voltage. The main features of this paper are listed below:

- The input current and voltage are globally estimated from the output voltage via a fifth-dimensional estimator. Unlike most methods, no *a priori* knowledge about the parasitic resistances and bounds on the states of the system is needed.
- The exponential stability of the estimator is guaranteed via Lyapunov analysis under a PE condition on the input control signal, which is ensured in normal operating conditions.
- The estimator, in conjunction with the controller, preserved the stability of the closed-loop system.
- Verification of the theoretical results is concluded via Processor-in-the-loop (PIL) studies done by OPAL-RT OP 5700.

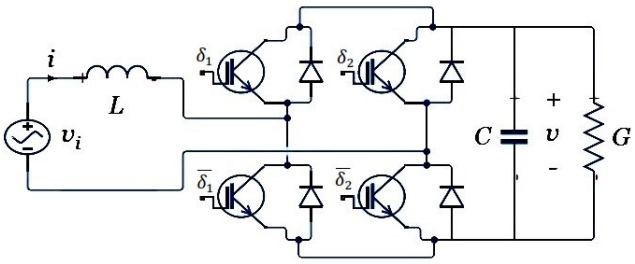

FIGURE 1. AC-DC full-bridge boost converter circuit.

The rest of the paper is organized as follows. Section II is devoted to the problem formulation. The main results of the paper are presented in Section III, where the I&I-based estimator is proposed, and its convergence is analyzed. The estimator is applied in Section IV for PFC purposes. The performance of the proposed scheme is evaluated using PIL results in Section V. Finally, the paper is concluded in Section VI.

II. PROBLEM FORMULATION

Consider the single-phase full-bridge boost converter shown in Fig. 1. The circuit of the converter combines two pairs of transistor-diode switches in two legs to form a bidirectional operation. The switches in the legs are controlled by a pulse width modulation (PWM) circuit in a complementary way *i.e.*, $\delta_1 = \bar{\delta}_2 := 1 - \delta_2$. The switch position function takes the values in the finite set $0, 1\}$, which provides two conduction states: $\delta_1 = \bar{\delta}_2$ in the on-state ($\delta_1 = \bar{\delta}_2 = 1$) and $\delta_1 = \bar{\delta}_2$ in the off-state ($\delta_1 = \bar{\delta}_2 = 0$). The dynamic equations describing the *average* behavior of the converter can be obtained using Kirchhoff's laws as [8]

$$L\frac{di}{dt} = -uv + v_i(t), \tag{1}$$

$$C\frac{dv}{dt} = ui - Gv, \tag{2}$$

where $i \in \mathbb{R}$ describes the current flows in the inductance L, and $v \in \mathbb{R}$ is the voltage across both the capacitance C and the load conductance G. The continuous signal $u \in [-1, 1]$, operates as a control input and is fed to the PWM circuit to generate the sequence of switching positions δ_1 and δ_2. The *switched model* can be obtained by standing $\delta_1 - \delta_2 = 2\delta_1 - 1$ as the control signal u in (1)-(2). Finally, $v_i(t)$ is the voltage of the AC line source which has the following form

$$v_i(t) = E\sin(\omega t + \rho), \tag{3}$$

where the real constants $E > 0$, $\omega > 0$, and ρ represent its amplitude, angular frequency, and phase, respectively.

As mentioned, the control objective can be achieved indirectly by stabilizing the input (inductor) current in phase with

the input voltage. This is done due to unstable zero dynamics with respect to the output to be regulated. In the following section, we deal with the effect of the phase difference between the input voltage and current on the waveform of the output voltage signal. To this end, let us assume that the input current has the following steady-state form

$$i_s(t) = I_s \sin(\omega t + \rho - \Delta\rho), \tag{4}$$

for some constant $\Delta\rho \in (-\pi/2, \pi/2)$ as the phase difference between the input voltage and current, and some $I_s > 0$ yet to be specified. Replacing (4) into (1) yields

$$u_s v_s = E \sin(\omega t + \rho) - L\omega I_s \cos(\omega t + \rho - \Delta\rho), \tag{5}$$

where u_s and v_s are the control input and output voltage in steady-state, respectively. Now, replacing (4) and (5) into (2) yields the following dynamics in steady-state

$$Cv_s\dot{v}_s + Gv_s^2 = EI_s \sin(\omega t + \rho)\sin(\omega t + \rho - \Delta\rho) - \frac{L\omega I_s^2}{2}\sin(2\omega t + 2\rho - 2\Delta\rho). \tag{6}$$

The steady-state solution of (6) can be calculated using Fourier series as follows

$$v_s^2(t) = \frac{EI_s}{2G}\cos(\Delta\rho) - \frac{Gd_1 - C\omega d_2}{G^2 + C^2\omega^2}\cos(2\omega t + 2\rho) - \frac{Gd_2 + C\omega d_1}{G^2 + C^2\omega^2}\sin(2\omega t + 2\rho), \tag{7}$$

with

$$d_1(\Delta\rho) := \frac{I_s}{2}(E\cos(\Delta\rho) - L\omega I_s \sin(2\Delta\rho)), \tag{8}$$

$$d_2(\Delta\rho) := \frac{I_s}{2}(E\sin(\Delta\rho) + L\omega I_s \cos(2\Delta\rho)). \tag{9}$$

Finally, doing a basic trigonometric simplification (7) takes the form

$$v_s^2(t) = \frac{EI_s}{2G}\cos(\Delta\rho) + A\sin(2\omega t + 2\rho + \varrho), \tag{10}$$

with

$$A(\Delta\rho) := \sqrt{\frac{d_1^2 + d_2^2}{G^2 + C^2\omega^2}}, \tag{11}$$

$$\varrho(\Delta\rho) := \arctan 2\left(\frac{Gd_1 - C\omega d_2}{Gd_2 + C\omega d_1}\right). \tag{12}$$

The new representation, given by (10), demonstrates the relationship between the phase difference and the steady-state amplitude of the input current and the second-order harmonic on the output. The solution in the presence of parasitic resistance in (1) with no phase difference in (4) has been obtained in [8] and [11].

Remark 1: The DC-component of v_s in steady-state can be concluded from (10) and is given by

$$V_s(\Delta\rho, I_s) = \sqrt{\frac{EI_s}{2G}\cos(\Delta\rho)}. \tag{13}$$

As a result, to provide the desired output voltage V_d, the input current amplitude must be forced to achieve

$$I_s(\Delta\rho) = \frac{2GV_d^2}{E\cos(\Delta\rho)}, \tag{14}$$

which justifies the fact that for any phase shift (positive or negative) the amplitude of input current and then the converter losses increases. For $\Delta\rho = 0$, the minimum value of I_s can be achieved and is defined as

$$I_0 := \frac{2GV_d^2}{E}. \tag{15}$$

As an example, consider the static control law in [11] which causes the following input current in steady-state

$$i_s(t) = \frac{I_0}{\sqrt{1+\alpha^2}}\sin(\omega t + \rho - \arctan(\alpha)), \tag{16}$$

with $\alpha = L\omega/KE$ for some constant $K > 0$. Replacing the amplitude and phase of the current in (13) yields to

$$V_s = \frac{V_d}{\sqrt{1+\alpha^2}}, \tag{17}$$

which indicates a steady-state error in the output voltage.

Remark 2: The minimum amplitude of the second-order harmonic $A(\Delta\rho)$ does not occur for $\Delta\rho = 0$. From (11) it can be computed that for $\Delta\rho$ which satisfies the following inequality

$$\frac{\sin^2(\Delta\rho)}{EL\omega I_0} < \frac{\sin(2\Delta\rho)(2\cos(\Delta\rho) - \cos(2\Delta\rho))}{E^2\cos^2(\Delta\rho) + L^2\omega^2 I_0^2(1 + \cos^2(\Delta\rho))}, \tag{18}$$

the magnitude of $A(\Delta\rho)$ is less than $A(0)$. From (18) it can be concluded that when the converter operates in leading form, *i.e.*, $\Delta\rho < 0$, the magnitude of $A(\Delta\rho)$ increases, but, it can be decreased when the converter operates in lagging form with a small $\Delta\rho$ near to zero. This may be induced by time delays or unmodeled dynamics in the actual system.

With respect to the remarks above which highlight the importance of phase difference in the output signal quality, in this paper we are interested to estimate the parameter vector

$$\theta := [\theta_1, \theta_2] =: [E\sin(\rho), E\cos(\rho)], \tag{19}$$

from the output voltage v. The amplitude and the phase can be obtained from the above vector as

$$E = |\theta| = \sqrt{\theta\theta}, \tag{20}$$

$$\rho = \arctan 2(\theta_1, \theta_2), \tag{21}$$

and the corresponding regressor can be defined as

$$\varphi(t) := \frac{1}{L}[\cos(\omega t), \sin(\omega t)], \tag{22}$$

to get

$$v_i(t) = L\varphi\theta = E\sin(\omega t + \rho). \tag{23}$$

III. ESTIMATOR DESIGN

In this section, an estimator is designed for the system (1)-(2) to estimate $v_i(t)$ and $i(t)$ from the output $v(t)$. In the design procedure, the following assumptions are considered.

Assumption 1: The system (1)-(2) is *forward complete*, *i.e.*, trajectories exist for all $t \in \mathbb{R}_+$.

Assumption 2: The measurable state is $v(t)$ but $i(t)$ is not measurable.

Assumption 3: The parameters ω, C, L and G are known but E, ρ and the parasitic resistances are not known *a priori*.

Assumption 4: The time derivative of the control signal u is available.

Assumption 5: The control signal u is continuous and persistently exciting ($u \in$ PE), that is, if

$$\int_t^{t+T} u^2(\tau)\, d\tau \geq \delta, \tag{24}$$

for some constants $\delta, T > 0$ and for all $t \in \mathbb{R}_+$.

The first assumption is standard in the estimator design and is extremely milder compared to the boundedness of trajectories. It is worth pointing out that this assumption practically holds due to the existence of the parasitic resistance in the input side (see Lemma 8.1 in [9]). Assumption 2 is attractive from the practical implementation viewpoint because it is easier to measure voltage in contrast to current. The third assumption relaxes the measuring of the input voltage and *a priori* knowledge about the parasitic resistances. Although Assumption 4 seems to be somewhat restrictive, a dynamic control law, like the one introduced in Proposition 8.9 of [9], satisfies this assumption. Assumption 5 is needed to make the input current i observable from the output voltage v. The assumption permits for a control signal sign changes that covers the AC-DC boost converters with a complete bidirectional bridge transistor-diode arrays (full-bridge) besides the traditional interleaved topologies formed from a *diode bridge* connected to a boost chopper. Regarding (5), the latter assumption is satisfied when the system draws a sinusoidal input current and the output voltage takes a real positive value.

Following [32], to form a proper adaptive structure, let us change the coordinate by the parameter-dependent transformation

$$\iota(t) := i(t) - \mu^{\mathsf{T}}(t)\,\theta, \tag{25}$$

where $\mu : \mathbb{R}_+ \to \mathbb{R}^2$ is an auxiliary signal whose dynamics yet to be specified. Now, the dynamics of the system (1)-(2) can be represented in terms of the unavailable variable $\iota(t)$ and θ as

$$\begin{bmatrix} \dot{\iota} \\ \dot{\theta} \end{bmatrix} = \begin{bmatrix} 0 & (\varphi - \dot{\mu})^{\mathsf{T}} \\ o_2 & O_2 \end{bmatrix} \begin{bmatrix} \iota \\ \theta \end{bmatrix} - \begin{bmatrix} \frac{u}{L} \\ o_2 \end{bmatrix} v, \tag{26}$$

$$\dot{v} = \frac{u}{C} \begin{bmatrix} 1 & \mu^{\mathsf{T}} \end{bmatrix} \begin{bmatrix} \iota \\ \theta \end{bmatrix} - \frac{G}{C} v, \tag{27}$$

where $o_2 \in \mathbb{R}^2$ and $O_2 \in \mathbb{R}^{2\times 2}$ are zero vector and matrix, respectively.

Proposition 1: Consider the system (1)-(2) verifying Assumption 1-5. Define the fifth-dimensional estimator

$$\begin{aligned} \begin{bmatrix} \dot{\zeta}_1 \\ \dot{\zeta}_2 \end{bmatrix} &= -\kappa \left(\frac{u}{C}\right)^2 \begin{bmatrix} 1 & -\lambda\mu^{\mathsf{T}} \\ \Lambda\mu\lambda & \Lambda\mu\lambda\mu^{\mathsf{T}} \end{bmatrix} \left(\begin{bmatrix} \zeta_1 \\ \zeta_2 \end{bmatrix} + \begin{bmatrix} 1 \\ \Lambda\mu\lambda \end{bmatrix} \frac{\kappa}{C} uv \right) \\ &\quad - \begin{bmatrix} \frac{u}{L} \\ o_2 \end{bmatrix} v + \begin{bmatrix} 1 \\ \Lambda\mu\lambda \end{bmatrix} \frac{\kappa}{C} \left(\frac{G}{C} u - \dot{u} \right) v - \begin{bmatrix} 0 \\ \Lambda\dot{\mu}\lambda \end{bmatrix} \frac{\kappa}{C} uv, \end{aligned} \tag{28}$$

$$\dot{\mu} = -\kappa \left(\frac{u}{C}\right)^2 \mu \left(1 + \lambda\right) + \varphi(t), \tag{29}$$

where κ and λ are positive constants, and $\Lambda = \Lambda \in \mathbb{R}^{2\times 2}$ is positive definite. Let

$$\bar{\iota}(t) := \iota(t) - \left(\zeta_1 + \frac{\kappa}{C} uv\right), \tag{30}$$

$$\bar{\theta}(t) := \theta - \left(\zeta_2 + \Lambda\mu\lambda \frac{\kappa}{C} uv\right). \tag{31}$$

I Then

$$\mu(t) \in \mathcal{L}_\infty, \bar{\iota}(t) \in \mathcal{L}_\infty, \bar{\theta}(t) \in \mathcal{L}_\infty, \tag{32}$$

$$u(t)\,\bar{\iota}(t) \in \mathcal{L}_2, u(t)\,\mu(t)\,\bar{\theta}(t) \in \mathcal{L}_2, \tag{33}$$

and if $\dot{u} \in \mathcal{L}_\infty$ we have

$$\lim_{\tau\to\infty} u(t)\,\bar{\iota}(t) = 0, \tag{34}$$

$$\lim_{\tau\to\infty} u(t)\,\mu^{\mathsf{T}}(t)\,\bar{\theta}(t) = 0, \tag{35}$$

II If Assumption 5 holds, then

$$\lim_{\tau\to\infty} \mathrm{e}^{\ell t}\bar{\iota}(t) = 0, \tag{36}$$

$$\lim_{\tau\to\infty} \mathrm{e}^{\ell t}\bar{\theta}(t) = 0, \tag{37}$$

for some constant $\ell > 0$.

Proof: Differentiating (30)-(31) and substituting (25), (28), and (29) therein, the dynamics of the estimation errors can be expressed in the following linear time-varying form

$$\begin{bmatrix} \dot{\bar{\iota}} \\ \dot{\bar{\theta}} \end{bmatrix} = -\kappa \left(\frac{u(t)}{C}\right)^2 \begin{bmatrix} 1 & -\lambda\mu^{\mathsf{T}}(t) \\ \Lambda\mu(t)\,\lambda & \Lambda\mu(t)\,\lambda\mu^{\mathsf{T}}(t) \end{bmatrix} \begin{bmatrix} \bar{\iota} \\ \bar{\theta} \end{bmatrix}. \tag{38}$$

Now, consider the Lyapunov function candidate

$$V(\bar{\eta}) = \frac{1}{2}\left(\bar{\iota}^2 + \bar{\theta}^{\mathsf{T}}\Lambda^{-1}\bar{\theta}\right), \tag{39}$$

whose time-derivative along the trajectories of (38) is given by

$$\dot{V} = -\kappa \left(\frac{u}{C}\right)^2 \left(\bar{\iota}^2 + \lambda \left|\mu^{\mathsf{T}}\bar{\theta}\right|^2\right), \tag{40}$$

which is nonpositive and implies that the system (38) has a uniformly globally stable equilibrium at the origin and consequently $V \in \mathcal{L}_\infty$, $\bar{\iota} \in \mathcal{L}_\infty$, and $\bar{\theta} \in \mathcal{L}_\infty$. Note that, for φ given in (22), all the trajectories of (29) are bounded regardless of the control input, *i.e.*, $\mu \in \mathcal{L}_\infty$ and consequently

$\dot{\mu} \in \mathcal{L}_\infty$. As a result, we have from (38) that $\dot{\bar{\iota}} \in \mathcal{L}_\infty$ and $\dot{\bar{\theta}} \in \mathcal{L}_\infty$. Using the above properties and recalling the assumption $\dot{u} \in \mathcal{L}_\infty$ we have that the time-derivative of the terms given in (33) are bounded. On the other hand, by integrating (40) it follows that

$$V(0) - V(\infty) = \kappa C^{-2} \int_0^\infty \left(u^2 \bar{\iota}^2 + \lambda \left| u\mu^\top \bar{\theta} \right|^2 \right) dt < \infty \tag{41}$$

which implies (33). Now, (34) and (35) follow directly by applying the alternative to Barbalat's Lemma reported in [33]. This completes the proof of part I.

Before establishing the proof of part II, notice that from (38) and (34)-(35) we get that $\dot{\bar{\iota}} \to 0$ and $\dot{\bar{\theta}} \to 0$ as $t \to \infty$. Now, recalling $u\bar{\iota} \in \mathcal{L}_2$ and (34), and invoking the assumed PE property of u in Assumption 5, the uniform asymptotic convergence of $\bar{\iota}$ to zero can be concluded directly from Lemma 1 in [34]. In similar way, using $u\mu^\top\bar{\theta} \in \mathcal{L}_2$ and (35), and invoking the lemma, $\bar{\theta}$ has the same convergence property if $u\mu^\top \in$ PE. Now, notice that, under Assumption 5, the origin of the unperturbed system (29), *i.e.*, (29) when $\varphi = 0$, is uniformly exponentially stable and consequently the perturbed system (29) is bounded-input to bounded-state stable with φ as the input. It is clear that the regressor vector φ given in (22) is PE and Thanks to Proposition 2 and Eq. (23) in [35], it can be concluded that $u\varphi^\top$ is PE for the regressor vector (22). Now, invoking the conservation of the PE property under filtering by an exponentially stable filter, the condition $u\mu^\top \in$ PE can be concluded. As a result, $\bar{\theta}$ converges to zero uniformly and asymptotically. The proof of the claim is completed by noting that, for linear time-varying systems, such as (38), uniform asymptotic stability confirms exponential stability by Theorem B.1.3 in [22]. □

Remark 3: If (36)-(37) hold, an exponent estimation of ι, θ, and i can be respectively obtained from, as

$$\hat{\iota} = \zeta_1 + \frac{\kappa}{C} uv, \tag{42}$$

$$\hat{\theta} = \zeta_2 + \Lambda\mu\lambda \frac{\kappa}{C} uv \tag{43}$$

$$\hat{i} = \hat{\iota} + \mu^\top \hat{\theta}, \tag{44}$$

where (25) has been used to get the last identity. Now, regarding (20)-(21), an asymptotic estimation of E and ρ can be obtained by

$$\hat{E} = \left| \hat{\theta} \right|, \tag{45}$$

$$\hat{\rho} = \arctan 2 \left(\hat{\theta}_1, \hat{\theta}_2 \right). \tag{46}$$

IV. ADAPTIVE OUTPUT FEEDBACK CONTROLLER

In this section, the dynamic controller proposed in Proposition 8.9 of [9] is used in conjunction with the proposed estimator to form an equivalent adaptive output feedback controller. The updated law of the control signal is given by

$$\dot{u} = \frac{1}{v} \left(-\frac{u^2}{C} i + w \right), \tag{47}$$

where $w(t)$ comes from the marginally stable filter

$$w(s) = k \frac{s^2 + as + b}{s^2 + \omega^2} e(s), \tag{48}$$

with some positive constants a, b, k, and

$$e := v_i - uv - L \frac{di_d}{dt} - K(i_d - i), \tag{49}$$

where K is a positive constant and $i_d(t) = I_0 \sin(\omega t + \rho)$ in which I_0 is given by (15). With respect to the analysis in Remark 1, the input current i_d results in an output voltage with V_d in average. It is shown in [9] and [11] that for sufficiently large k, the closed-loop system is asymptotically stable and i converges to i_d for all trajectories satisfying $v \in \mathbb{R}_{>0}$. As a result, with respect to (5), it can be concluded that u is a sinusoid signal in the steady-state and Assumption 5 is satisfied.

Remark 4: By substituting $v_i = v_{ac} - ri_d$ in (49), the exact expression of the controller [11] can be obtained where v_{ac} is the source voltage and $r > 0$ is the parasitic resistance which is employed to model the power dissipation regarding to the parasitic resistive effects of the inductor and the impedance concerning the switches and source. Due to i_d is in phase with v_{ac}, we can incorporate its effect on the amplitude of v_i (see equation (23) and Remark 8 both in [11]).

Note that, the feedforward and the feedback terms in (49) indicate the importance of an accurate estimation of the input current and voltage. An equivalence adaptive output feedback control law can be constructed by replacing the state i and the parameters E and ρ with their respective estimates $\hat{i}$, $\hat{E}$ and $\hat{\rho}$ given by (44), (45) and (46), respectively. Notice that, with respect to (15), singularity problem can occur when $\hat{E}$ is replaced to estimate I_0 in i_d. In order to remove the problem, we assume that E^{-1} is incorporated in the arbitrary gain k and the signal

$$\varepsilon(t) := Ee(t), \tag{50}$$

is injected to the (48) instead of $e(t)$. Now, an estimate for $\varepsilon(t)$ can be achieved by

$$\hat{\varepsilon} = \hat{E} \left(K\hat{i} - uv \right) - 2L\omega G V_d^2 \cos(\omega t + \hat{\rho}) + \left(\hat{E}^2 - 2KGV_d^2 \right) \sin(\omega t + \hat{\rho}), \tag{51}$$

which provides

$$\hat{w}(s) = d \frac{s^2 + as + b}{s^2 + \omega^2} \hat{\varepsilon}(s). \tag{52}$$

where d is related to k in (48) with $d = k/E$. Now, the connection between the control algorithm and the system will be completed by

$$\dot{u} = \frac{1}{v} \left(-\frac{u^2}{C} \hat{i} + \hat{w} \right). \tag{53}$$

Remark 5: Asymptotic stability of the closed-loop system can be dealt with invoking cascade theorem. To this end, the existence of the parasitic resistance in practice ensures

boundedness of the system trajectories regardless of u with respect to Lemma 8.1 in [9]. As a result, the trajectories of the system in closed loop with (53) remain bounded provided $v \in \mathbb{R}_{>0}$. The closed-loop system can be considered as a nominal asymptotic stable system (system (1)-(2) with (47) as control law) perturbed by the estimation errors $\tilde{i}$, $\tilde{E}$, and $\tilde{\rho}$. From Proposition 1 and Remark 3, it can be concluded that the perturbation term asymptotically converges to zero provided $u \in$ PE. Now, all trajectories satisfying $v \in \mathbb{R}_{>0}$ are bounded and asymptotic convergence of the overall system for sufficiently large k and $u \in$ PE can be concluded from Lemma 2.1 in [36].

Remark 6: From a practical viewpoint, the inductance, capacitance and conductance values could be dramatically changed according to the current and voltage. From the estimator dynamics (28)-(29) and the controller dynamics (51)-(53), such uncertainties in the values of the parameters could be model in the dynamics as an additive disturbance which depends upon to the system states. Regarding to the dynamics of the unperturbed estimator and closed-loop system are exponentially and uniformly asymptotically stable, respectively, boundedness of the estimation and tracking errors are guaranteed for bounded disturbances by total stability arguments.

V. SIMULATION AND PROCESSOR-IN-THE-LOOP RESULTS

Fig. 2 shows the rectifier control block diagram that includes the proposed estimator. Simulation and processor-in-the-loop results are performed with the system parameters and the estimator-controller gains are listed in Table 1 and Table 2, respectively. The system and controller parameters are borrowed from the experimental setup in [11] for comparison purposes. All initial values of the controller and estimator are set to zero. The switching frequency of the PWM is set to 10 kHz. The results of this section are decomposed in two simulation and laboratory tests. The simulation tests deal with the robustness of the proposed estimator and controller in the presence of uncertainty in inductance, capacitance, and conductance values. The laboratory tests intend to assess the adaptive performance of the proposed control system in confronting with step changes in the amplitude and phase of AC-source, and the desired output voltage.

A. SIMULATION RESULTS

In this subsection, the simulations were carried out via the Simulink® of MATLAB® R2017b to assess the performance of the control system for the uncertainty in L, C, G, and ω. To this end, 25% uncertainty appears on L in the interval $t = 0.2$ to 0.4 sec, on C in the interval $t = 0.6$ to 0.8 sec, and on G in the interval $t = 1$ to 1.2 sec. Finally, 2% frequency is dropped in the interval $=$ 1.4 to 1.6 sec. Along the test, the desired output is set to $V_d = 200$ V. Fig. 3 plots the time histories of the output voltage. Fig. 4-8 plot the time histories of the input voltage and current estimations. The time history of the power factor is shown in Fig. 9.

TABLE 1. Parameters of the system used in PIL studies parameter value unit.

Parameter	Value	Unit
E	150	V
ω	100π	rad/sec
ρ	0	rad
r	2.2	Ω
L	2.13	mH
C	1100	μF
G	1/87	S

Fig. 4 shows the transient behavior of the estimator which illustrates the estimated signals $\hat{v}_i$ and $\hat{i}$ converge to their real values fast from zero-initial condition. As mentioned in Remark 4, regarding to the presence of the parasitic resistance, a voltage drop appears in v_i, so the amplitude of the waveform is less than E. From Fig. 3 and 5, we can conclude that the controller and estimator have a robust performance against the inductance uncertainty along the test. When the uncertainty in capacitance is applied to the test, the controller behavior shows a small deviation in Fig. 3, whereas Fig. 6 shows the estimator is working in high accuracy. So, it can be concluded that the estimator has a robust performance against the capacitance uncertainty but the controller is sensitive to the change along the test. Also, Fig. 3 shows 5% (10 V) steady-state error in the DC-link voltage when uncertainty in the load is applied. As shown in Fig. 7, the estimator, with a high accuracy, estimates the input voltage signal whereas estimation of the input current shows a deviation in the signal amplitude for this change. Regarding to the high accuracy estimation of the input voltage in Fig. 5-7, it can be concluded that $\hat{E}$ and $\hat{\rho}$ have robustness against the changes in the circuit elements. As shown in Fig. 3 and 8, both the controller and estimator illustrate more sensitive behaviour to the frequency drop than the changes in L, C, and G. Fig. 8 shows that the frequency drop causes a phase deviation in the current estimation. However, the estimated input voltage is well synchronized with the actual one by the adaptive part of the estimator during the tests. This makes it possible to achieve the control objective on the input side, *i.e.*, unity power factor, with high accuracy, as shown in Fig. 9.

B. PROCESSOR-IN-THE-LOOP RESULTS

The laboratory setup including OPAL-RT OP 5700 and power quality analyzer, which is employed to support the theoretical results, is shown in Fig. 10. The rectifier runs in FPGA of OPAL-RT. The CPU of OPAL-RT is used to implement the controller and estimator in the discrete domain. The evaluation is done by computing the DC error of the output voltage, and the harmonic characteristics of the input current such as total harmonic distortion (THD), displacement angle, and power factor.

Fig. 11 shows the steady-state performance of the proposed adaptive output feedback controller in tracking $V_d = 200$ V. The PIL results are gathered in Table 3. According to this

TABLE 2. Estimator & controller gains gain value.

Gain	Value
a	1200
b	200000
d	4600/15
K	15
κ	0.00017
Λ	$5 \times I_2$
λ	80

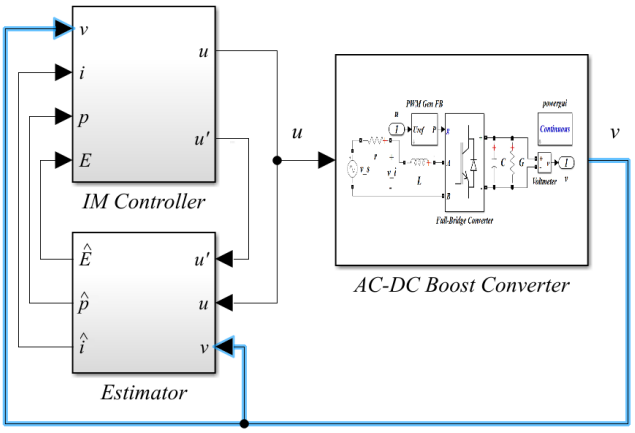

FIGURE 2. Block diagram of the control system describing the connection between the estimator, the controller and the converter.

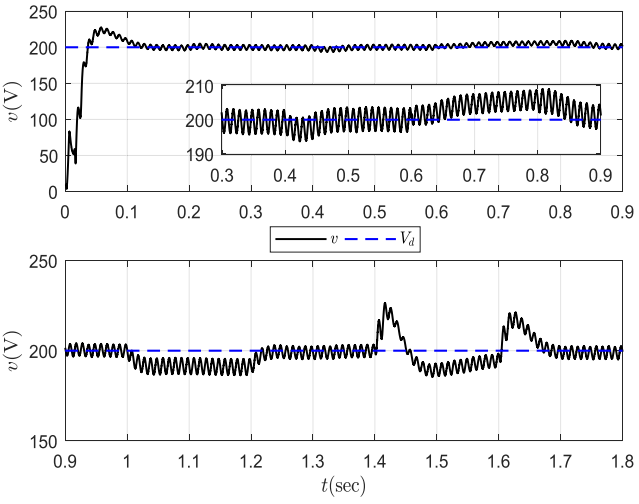

FIGURE 3. Response of the control system to 25% uncertainties in L for t:0.2:0.4 sec, in C for t:0.6:0.8 sec, in G for t:1:1.2 sec, and 2% frequency drop for t:1.4:1.6 sec.

TABLE 3. Harmonic analysis.

DC Error (V)	Displacement (°)	THD (%)	Power Factor
0.39	0.0111	4.8	0.9991

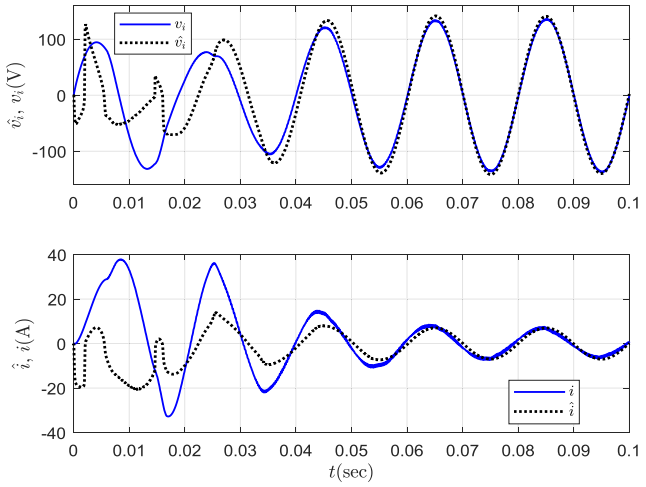

FIGURE 4. Response of the estimator at the start time.

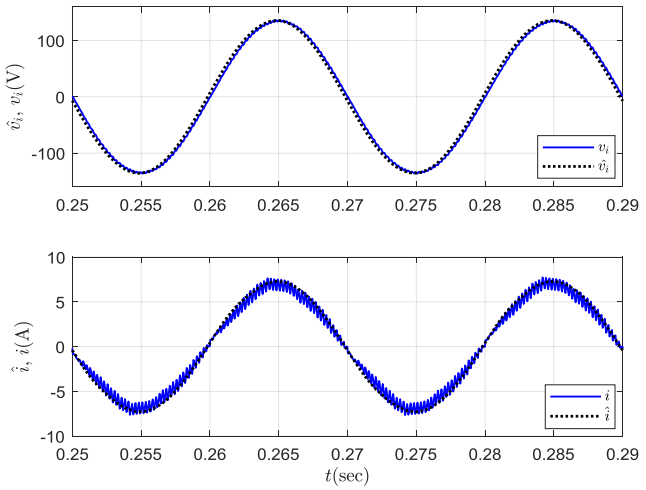

FIGURE 5. Response of the estimator to 25% uncertainty in the inductance value at steady-state.

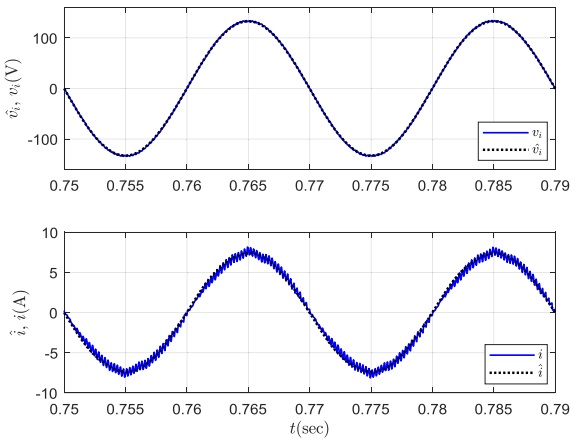

FIGURE 6. Response of the estimator to 25% uncertainty in the capacitance value at steady-state.

table, the control objectives have been achieved with a high accuracy. The harmonic content of the input current is illustrated in Fig. 12 which presents a comparable result with the adaptive state feedback controllers reported in [11]. Also, comparing with the harmonic limits specified by European standard EN61000-3-2 reported in [37] Fig. 12 demonstrates that the proposed control algorithm obeys the standard with a

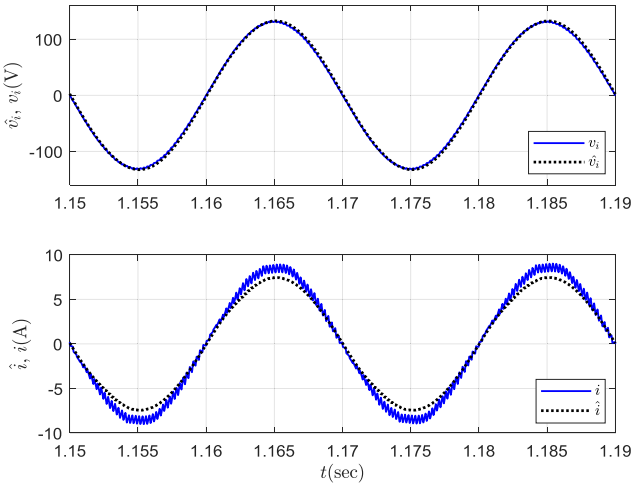

FIGURE 7. Response of the estimator to 25% uncertainty in the conductance value at steady-state.

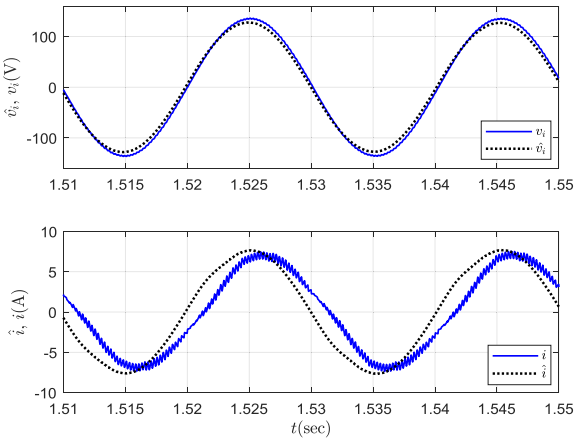

FIGURE 8. Response of the estimator to 2% frequency drop at steady-state.

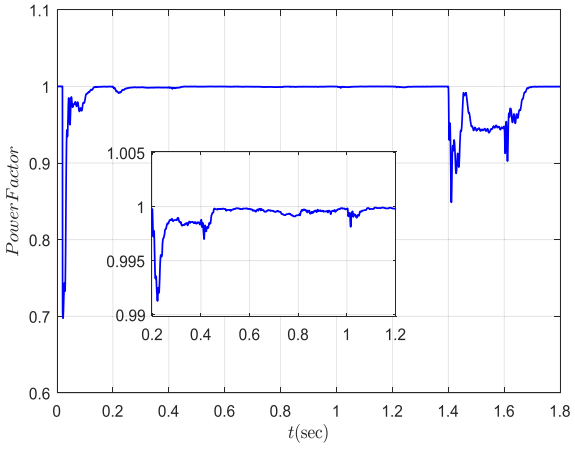

FIGURE 9. Power factor history along the test.

large margin. The proposed estimator presents a lower THD owing to providing a smooth estimation of the input current that is required in all the CMC strategies to stabilize the

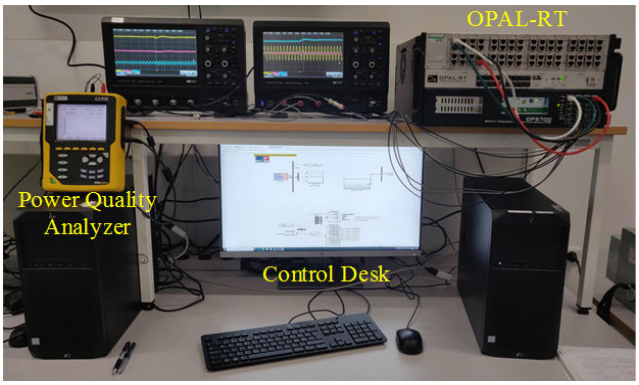

FIGURE 10. Experimental setup based on OP5700.

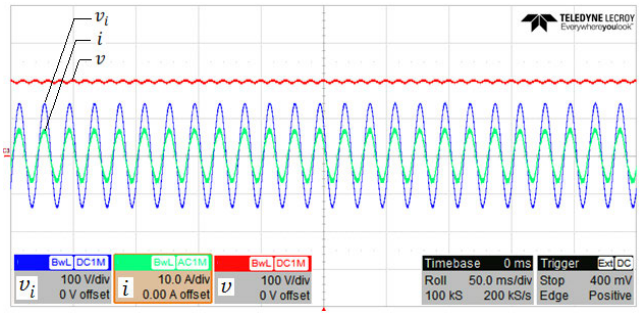

FIGURE 11. Time histories of v, v_i and i in steady-state.

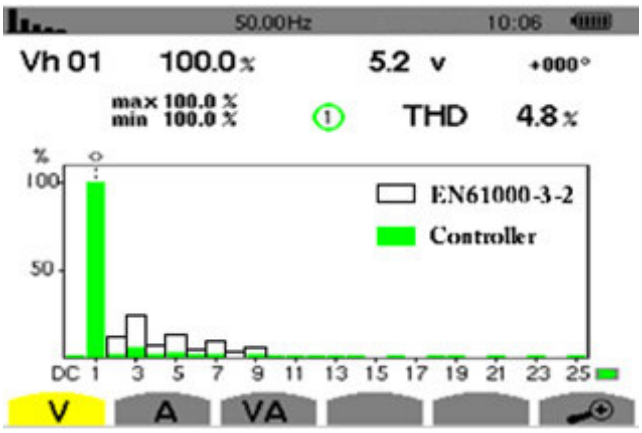

FIGURE 12. Fourier spectrum of the input current harmonics for the proposed control algorithm compared to the standard EN61000-3-2.

tracking error dynamics. The best performance of the CMC controllers proposed in [11] associated with THD, power factor, displacement and DC error are obtained by the Passivity Based (PB) controller with 5.4%, the PB controller with 0.9981, the adaptive Feedback Linearization (FL) controller with 0° and the adaptive Internal Model (IM) controller with 0.04 V, respectively (see the Table 4 in [11]). In comparison, Table 3 shows that the overall performance of the proposed adaptive output feedback controller is comparable with the control strategies proposed in [11].

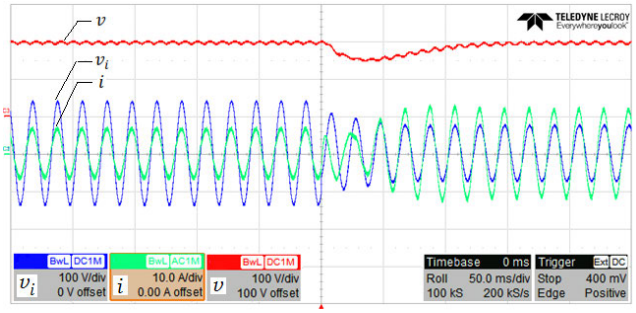

FIGURE 13. Time responce of v and i to a step change in the amplitude of v_i from 150 to 100 V.

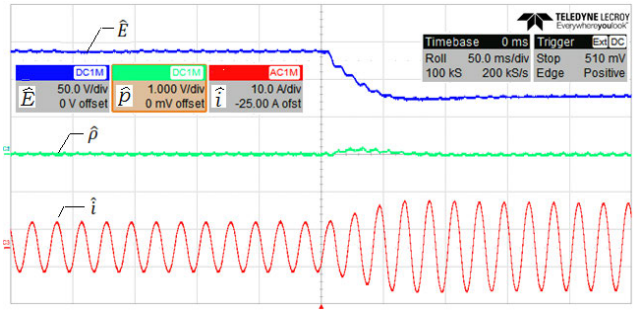

FIGURE 14. Time histories of $\hat{E}$, $\hat{\rho}$ and $\hat{i}$ to a step change in the amplitude of v_i from 150 to 100 V.

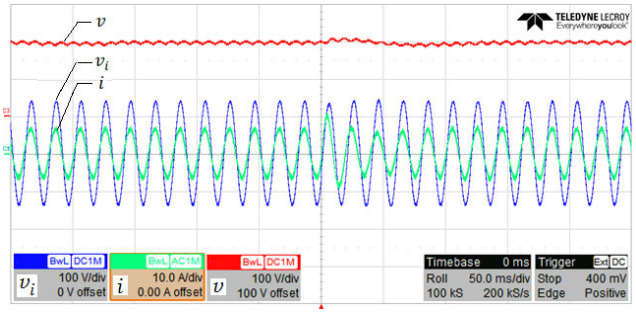

FIGURE 15. Time responce of v and i to a step change in the phase of v_i from 0 to 10 deg.

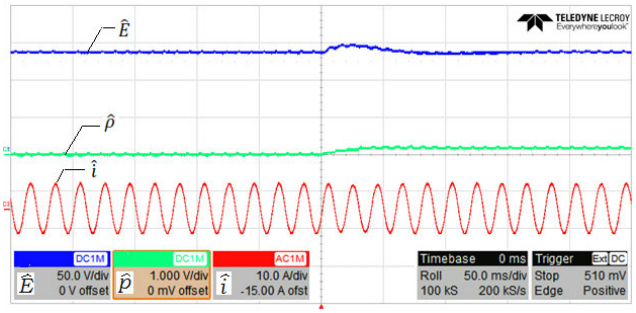

FIGURE 16. Time histories of $\hat{E}$, $\hat{\rho}$ and $\hat{i}$ to a step change in the phase of v_i from 0 to 10 deg.

Fig. 13 and 14 respectively display the response of the proposed control system and the estimator to the change in E from 150 to 100 V. By this change and at the beginning, the output voltage v drops and then after 0.15 sec, the proposed scheme has quickly damped the voltage deviation and gives a satisfactory performance dealing with the server changes in the input voltage. Notice that Fig. 14 shows the estimator tracks a smaller value than E, due to the consideration of the parasitic resistance in the laboratory tests. This drop becomes bigger when the input current increases after the step-down change in the input voltage. The laboratory results for the case of the known parameters in [11], shows a significant steady-state tracking error. The comparison emphasizes the importance of adaptation role on E in the proposed estimator.

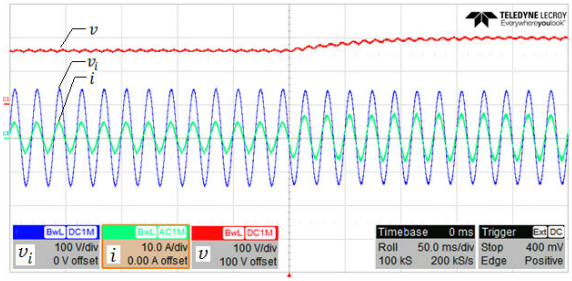

FIGURE 17. Time response of v, v_i and i to a step change in V_d from 160 to 200 V.

Fig. 15 and 16 illustrate the response of the control system to the phase change in the input voltage from 0° to 10°. Obtained results represent a fast convergence in the estimator and controller performance. As can be seen in Fig. 16, the estimator has been able to synchronize the estimated signals to the new one after 0.05 sec. Fig. 17 plots the response of the control system to a step-change in the desired output from 160 to 200 V. It shows that the output voltage reaches to its new reference without overshoot after 0.1 sec.

VI. CONCLUSION

In this paper, the impact of the phase difference between the input voltage and current on the quality of the output voltage signal has been extensively studied. The mathematical analyses clearly demonstrate that larger values of the phase shift result in increased DC error and higher amplitude of harmonics in the output voltage. To address this issue, a novel nonlinear, globally exponentially convergent and robust estimator has been developed using I&I-based filtered transformation. By employing a fifth-dimensional estimator, the input current and voltage are accurately estimated from the output voltage. In addition, an application of the estimator has been presented in conjunction with a dynamic controller. Laboratory tests illustrate a fast convergence and robust performance of the proposed scheme. Our future study concentrates the extinction of the proposed strategy on other widely used converters.

AKNOWLEDGMENT

The authors would like to express their appreciation for the support of Energi Fyn's Development Foundation for the OPAL-RT setup used for extracting the results in the Control and Protection at the Smart Grids Laboratory, University of Southern Denmark, Odense, Denmark.

REFERENCES

[1] X. Lu, J. M. Guerrero, K. Sun, J. C. Vasquez, R. Teodorescu, and L. Huang, "Hierarchical control of parallel AC–DC converter interfaces for hybrid microgrids," *IEEE Trans. Smart Grid*, vol. 5, no. 2, pp. 683–692, Mar. 2014.

[2] M. Najafzadeh, R. Ahmadiahangar, O. Husev, I. Roasto, T. Jalakas, and A. Blinov, "Recent contributions, future prospects and limitations of interlinking converter control in hybrid AC/DC microgrids," *IEEE Access*, vol. 9, pp. 7960–7984, 2021.

[3] S. Beheshtaein, R. M. Cuzner, M. Forouzesh, M. Savaghebi, and J. M. Guerrero, "DC microgrid protection: A comprehensive review," *IEEE J. Emerg. Sel. Topics Power Electron.*, early access, Mar. 12, 2019, doi: 10.1109/JESTPE.2019.2904588.

[4] A. M. Bouzid, J. M. Guerrero, A. Cheriti, M. Bouhamida, P. Sicard, and M. Benghanem, "A survey on control of electric power distributed generation systems for microgrid applications," *Renew. Sustain. Energy Rev.*, vol. 44, pp. 751–766, Apr. 2015.

[5] G. Cimini, M. L. Corradini, G. Ippoliti, G. Orlando, and M. Pirro, "Passivity-based PFC for interleaved boost converter of PMSM drives," *IFAC Proc. Volumes*, vol. 46, no. 11, pp. 128–133, 2013.

[6] G. Calisse, G. Cimini, L. Colombo, A. Freddi, G. Ippoliti, A. Monteriù, and M. Pirro, "Development of a smart LED lighting system: Rapid prototyping scenario," in *Proc. IEEE 11th Int. Multi-Conf. Syst., Signals Devices (SSD)*, Feb. 2014, pp. 1–6.

[7] R. Samani, D. Shekari, H. Pahlevani, and M. Pahlevani, "A multi-output AC/DC converter for LED grow lights," in *Proc. IEEE Energy Convers. Congr. Expo. (ECCE)*, Sep. 2018, pp. 4707–4711.

[8] G. Escobar, D. Chevreau, R. Ortega, and E. Mendes, "An adaptive passivity-based controller for a unity power factor rectifier," *IEEE Trans. Control Syst. Technol.*, vol. 9, no. 4, pp. 637–644, Jul. 2001.

[9] A. Astolfi, D. Karagiannis, and R. Ortega, *Nonlinear and Adaptive Control With Applications*. New York, NY, USA: Springer, 2007.

[10] R. Cisneros, M. Pirro, G. Bergna, R. Ortega, G. Ippoliti, and M. Molinas, "Global tracking passivity-based PI control of bilinear systems: Application to the interleaved boost and modular multilevel converters," *Control Eng. Pract.*, vol. 43, pp. 109–119, Oct. 2015.

[11] D. Karagiannis, E. Mendes, A. Astolfi, and R. Ortega, "An experimental comparison of several PWM controllers for a single-phase AC–DC converter," *IEEE Trans. Control Syst. Technol.*, vol. 11, no. 6, pp. 940–947, Nov. 2003.

[12] S. I. J. Seleme, L. M. F. Morais, A. H. R. Rosa, and L. A. B. Torres, "Stability in passivity-based boost converter controller for power factor correction," *Eur. J. Control*, vol. 19, no. 1, pp. 56–64, Jan. 2013.

[13] J. G. Hwang, P. W. Lehn, and M. Winkelnkemper, "A generalized class of stationary frame-current controllers for grid-connected AC–DC converters," *IEEE Trans. Power Del.*, vol. 25, no. 4, pp. 2742–2751, Oct. 2010.

[14] G. C. Konstantopoulos and Q. Zhong, "Nonlinear control of single-phase PWM rectifiers with inherent current-limiting capability," *IEEE Access*, vol. 4, pp. 3578–3590, 2016.

[15] D. del Puerto-Flores, J. M. A. Scherpen, M. Liserre, M. M. J. de Vries, M. J. Kransse, and V. G. Monopoli, "Passivity-based control by series/parallel damping of single-phase PWM voltage source converter," *IEEE Trans. Control Syst. Technol.*, vol. 22, no. 4, pp. 1310–1322, Jul. 2014.

[16] J. Lu, S. Golestan, M. Savaghebi, J. C. Vasquez, J. M. Guerrero, and A. Marzabal, "An enhanced state observer for DC-link voltage control of three-phase AC/DC converters," *IEEE Trans. Power Electron.*, vol. 33, no. 2, pp. 936–942, Feb. 2018.

[17] J. Lu, M. Savaghebi, A. M. Y. M. Ghias, X. Hou, and J. M. Guerrero, "A reduced-order generalized proportional integral observer-based resonant super-twisting sliding mode control for grid-connected power converters," *IEEE Trans. Ind. Electron.*, vol. 68, no. 7, pp. 5897–5908, Jul. 2021.

[18] J. Liu, S. Vazquez, L. Wu, A. Marquez, H. Gao, and L. G. Franquelo, "Extended state observer-based sliding-mode control for three-phase power converters," *IEEE Trans. Ind. Electron.*, vol. 64, no. 1, pp. 22–31, Jan. 2017.

[19] A. Mallik and A. Khaligh, "Control of a three-phase boost PFC converter using a single DC-link voltage sensor," *IEEE Trans. Power Electron.*, vol. 32, no. 8, pp. 6481–6492, Aug. 2017.

[20] G. Cimini, G. Ippoliti, G. Orlando, and M. Pirro, "Sensorless power factor control for mixed conduction mode boost converter using passivity-based control," *IET Power Electronics*, vol. 7, no. 12, pp. 2988–2995, 2014.

[21] R. Gavagsaz-Ghoachani, M. Phattanasak, J. Martin, B. Nahid-Mobarakeh, S. Pierfederici, and P. Riedinger, "Observer and Lyapunov-based control for switching power converters with LC input filter," *IEEE Trans. Power Electron.*, vol. 34, no. 7, pp. 7053–7066, Jul. 2019.

[22] R. Marino and P. Tomei, *Nonlinear Control Design: Geometric, Adaptive and Robust*. Upper Saddle River, NJ, USA: Prentice-Hall, 1996.

[23] M. Pahlevani, S. Pan, S. Eren, A. Bakhshai, and P. Jain, "An adaptive nonlinear current observer for boost PFC AC/DC converters," *IEEE Trans. Ind. Electron.*, vol. 61, no. 12, pp. 6720–6729, Dec. 2014.

[24] E. Panteley, R. Ortega, and P. Moya, "Overcoming the detectability obstacle in certainty equivalence adaptive control," *Automatica*, vol. 38, no. 7, pp. 1125–1132, Jul. 2002.

[25] M. Tavan, K. Sabahi, A. Hajizadeh, M. N. Soltani, and K. Jessen, "Overcoming the detectability obstacle in adaptive output feedback control of DC–DC boost converter with unknown load," *IEEE Trans. Control Syst. Technol.*, vol. 29, no. 6, pp. 2678–2686, Nov. 2021.

[26] M. Tavan, K. Sabahi, A. Hajizadeh, M. Soltani, and M. Savaghebi, "Output feedback control of DC–DC converters with unknown load: An application of I&I based filtered transformation," in *Proc. 60th IEEE Conf. Decis. Control (CDC)*, Austin, TX, USA, Dec. 2021, pp. 4725–4729.

[27] J. Moreno-Valenzuela and J. Guzman-Guemez, "Experimental evaluations of voltage regulators for a saturated boost DC-to-DC power converter," *Trans. Inst. Meas. Control*, vol. 38, no. 3, pp. 327–337, Mar. 2016.

[28] W. He, M. M. Namazi, T. Li, and R. Ortega, "A state observer for sensorless control of power converters with unknown load conductance," *IEEE Trans. Power Electron.*, vol. 37, no. 8, pp. 9187–9199, Aug. 2022.

[29] X. Zhang, M. Martinez-Lopez, W. He, Y. Shang, C. Jiang, and J. Moreno-Valenzuela, "Sensorless control for DC–DC boost converter via generalized parameter estimation-based observer," *Appl. Sci.*, vol. 11, no. 16, p. 7761, Aug. 2021.

[30] J. Liu, S. Laghrouche, and M. Wack, "Observer-based higher order sliding mode control of power factor in three-phase AC/DC converter for hybrid electric vehicle applications," *Int. J. Control*, vol. 87, no. 6, pp. 1117–1130, Jun. 2014.

[31] M. Tavan, K. Sabahi, and A. Hajizadeh, "A filtered transformation via dynamic matrix to state and parameter estimation for a class of second order systems," *Int. J. Control, Autom. Syst.*, vol. 17, no. 9, pp. 2242–2251, Sep. 2019.

[32] M. Tavan, A. Khaki-Sedigh, M.-R. Arvan, and A.-R. Vali, "Immersion and invariance adaptive velocity observer for a class of Euler–Lagrange mechanical systems," *Nonlinear Dyn.*, vol. 85, no. 1, pp. 425–437, Jul. 2016.

[33] G. Tao, "A simple alternative to the Barbalat lemma," *IEEE Trans. Autom. Control*, vol. 42, no. 5, p. 698, May 1997.

[34] R. Ortega and A. Fradkov, "Asymptotic stability of a class of adaptive systems," *Int. J. Adapt. Control Signal Process.*, vol. 7, no. 4, pp. 255–260, Jul. 1993.

[35] A. A. Bobtsov, A. A. Pyrkin, R. Ortega, S. N. Vukosavic, A. M. Stankovic, and E. V. Panteley, "A robust globally convergent position observer for the permanent magnet synchronous motor," *Automatica*, vol. 61, pp. 47–54, Nov. 2015.

[36] A. Loría and E. Panteley, "2 Cascaded nonlinear time-varying systems: Analysis and design," in *Advanced Topics in Control Systems Theory*. London, U.K.: Springer, 2005, pp. 23–64.

[37] *PFC Harmonic Current Emissions—Guide to EN61000-3-2:2014*, EPSMA Tech. Committee, EPSMA, Little Haseley, Oxfordshire, U.K., 2018.

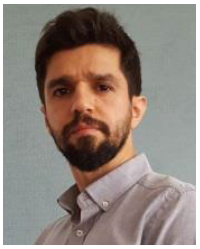

MEHDI TAVAN received the B.S. degree in electrical and electronic engineering from Mazandaran University, Babol, Iran, in 2007, and the M.S. and Ph.D. degrees (Hons.) in control systems engineering from Islamic Azad University, Science and Research Branch, Tehran, Iran, in 2011 and 2016, respectively.

He has been an Assistant Professor with the Department of Electrical Engineering, Islamic Azad University, Mazandaran, Nour and Mahmudabad, Iran. His current research interest includes nonlinear estimation and control, with special emphasis on applications.

KAMRAN SABAHI received the B.Sc. degree in electrical engineering from Ardabil University, Iran, in 2006, the M.Sc. degree in electrical engineering from the K. N. Toosi University of Technology, Iran, in 2008, and the Ph.D. degree from the University of Tabriz, Iran, in 2016.

In 2015, he was a Guest Ph.D. Student with the Department of Electrical Engineering, Harbin Institute of Technology, Harbin, China. From 2016 to 2019, he was an Assistant Professor with the Department of Electrical Engineering, Islamic Azad University Mamaghan, Iran. He is currently an Assistant Professor with the Department of Engineering Sciences, Faculty of Advanced Technologies, University of Mohaghegh Ardabili, Namin, Iran. His current research interests include the control of power systems, soft computing, and time-delay control systems. He is a reviewer of several IEEE, Elsevier, Springer, and IET journals.

MAHDI SHAHPARASTI (Senior Member, IEEE) received the Ph.D. degree in electrical engineering from Tarbiat Modares University, Tehran, Iran, in 2014. From 2015 to 2021, he was a Postdoctoral Researcher with the Technical University of Catalonia, Barcelona, and the University of Southern Denmark.

He is currently an Assistant Professor with the School of Technology and Innovations, University of Vaasa. His research interests include hardware design, control, stability, and dynamic analysis of power electronic systems, renewable energy resources, and motor drive systems.

AMIN HAJIZADEH (Senior Member, IEEE) received the M.S. and Ph.D. degrees (Hons.) in electrical engineering from the K. N. Toosi University of Technology, Tehran, Iran, in 2005 and 2010, respectively.

From 2014 to 2016, he was a Postdoctoral fellow with the Norwegian University of Science and Technology, Trondheim, Norway. Since 2016, he has been an Associate Professor with the Department of Energy Technology, Aalborg University, Denmark. His current research interests include the control of distributed energy resources, design, and control of power electronic converters for microgrid, and marine power systems. He is a member of scientific program committees of several IEEE conferences. He is also a reviewer of several IEEE and IET journals, and the guest editor and an associate editor for several special issues in IEEE, IET, and Elsevier.

MOHSEN SOLTANI (Senior Member, IEEE) received the M.Sc. degree in electrical engineering from the Sharif University of Technology, Tehran, Iran, in 2004, and the Ph.D. degree in electrical and electronic engineering from Aalborg University, Aalborg, Denmark, in 2008.

He was a Visiting Researcher with the Eindhoven University of Technology, Eindhoven, The Netherlands, in 2007. From 2008 to 2012, he fulfilled a Postdoctoral and an Assistant Professor Program with Aalborg University. In 2010, he was a Visiting Scholar with Stanford University, Stanford, CA, USA. Since 2012, he has been an Associate Professor with the Department of Energy Technology, Aalborg University. In 2015, he completed a research leadership training program with Harvard Business School, Boston, MA, USA. Some of his recent projects involve modeling, control, and estimation in power electronics systems, microgrid, and offshore wind systems. His research interests include modeling, control, optimization, estimation, and fault detection and their applications to electromechanical and energy conversion systems, power electronics, wind turbines, and wind farms.

MEHDI SAVAGHEBI (Senior Member, IEEE) received the B.Sc. degree in electrical engineering from the University of Tehran, Iran, in 2004, and the M.Sc. and Ph.D. degrees in electrical engineering from the Iran University of Science and Technology, Tehran, in 2006 and 2012, respectively. From 2014 to 2017, he was a Postdoctoral Fellow with the Department of Energy, Aalborg University, where he was an Associate Professor, from 2017 to 2018. For the next four years, he was an Associate Professor and the Research Team Leader with the University of Southern Denmark, Odense, Denmark. Since June 2022, he has been an Associate Professor and the Leader of the Electric Energy Group, Department of Engineering Technology, Technical University of Denmark (DTU), Ballerup, Denmark. His research interests include renewable energy systems, microgrids, power quality, and the protection of electrical systems. He was the Guest Editor for Special Issue on Power Quality in Smart Grids-IEEE TRANSACTIONS ON SMART GRID and Special Issue on Power Quality and Protection in Renewable Energy Systems and Microgrids-*IET Renewable Power Generation*. He is a member of the Technical Committee on Renewable Energy Systems and Technical Committee on Smart Grids, IEEE Industrial Electronics Society.